

NEW INSIGHTS INTO THE EJECTA MASS-VELOCITY DISTRIBUTION: EXPERIMENTAL TIME-RESOLVED MEASUREMENTS AND APPLICATIONS TO CRATERING. B. Hermalyn¹, P. H. Schultz², K. J. Meech¹, and J. Kleya¹, ¹NASA Astrobiology Institute/Institute for Astronomy, University of Hawaii, Honolulu, HI (hermalyn@hawaii.edu); ²Brown University, Providence, RI.

Introduction: The mass ejected by impact events controls the distribution, provenance, and appearance of deposits across planetary surfaces. This ejecta mass-velocity distribution can also reveal fundamental aspects of the cratering process itself, e.g., proportional vs. non-proportional growth, excavation depths, and coupling. The distribution, particularly during the early-time, high-speed regime, is also important for interpreting recent observations of planned impact missions (e.g., Deep Impact and LCROSS), observed impacts onto planetary bodies (such as the event on A2/Linear [1,2]), and assessment of ejecta hazards for future rovers and astronauts. Direct measurement of materials ejected at early times is challenging to constrain experimentally due to their high speed (and thus considerable ballistic range) and relatively low mass. Previous studies have constrained the ejected mass through dimensional analysis [3], physical dissection [4,5,6], and experimental capture [7]. Here, we present preliminary results of the early to mid-stage mass-velocity distributions for impacts into granular media targets using a novel noninvasive imaging technique.

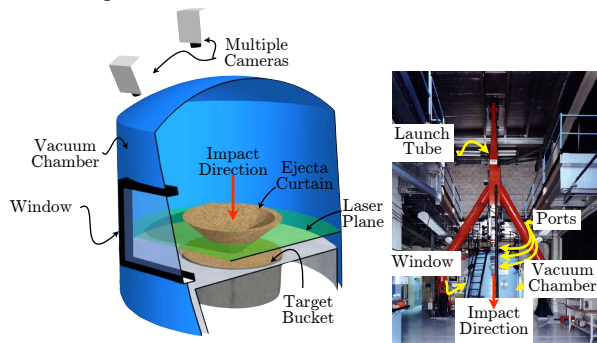


Figure 1. Schematic of experimental setup (left) and photo of AVGR (right). A laser light sheet is projected into the chamber parallel to the target surface to illuminate cross-sectional wedges of the ejecta curtain. High-speed cameras view the impact from above through windows in the vacuum chamber.

Experimental Methodology: In order to address and constrain the time-resolved ejecta mass-velocity distribution, a suite of impact experiments into #20-30 sand was carried out at the NASA Ames Vertical Gun Range (AVGR) to concurrently measure both mass and velocity. Here we present the results from 90° (vertical) impacts of 6.35mm diameter aluminum

projectiles. The technique employed in this study is an outgrowth of the initial work at the AVGR by [e.g., 8,9]. The method developed for this application (High-Speed Two-Frame Hybrid 3-Dimensional Particle Tracking Velocimetry, or “3D-PTV” in this work) appears qualitatively similar to the experimental setup previously employed by Anderson and Schultz, but the strategy for measurement differs due to the requirements of the high speed dataset and resolution needed for temporal description [10].

The 3D-PTV system utilizes a pulsed laser light sheet projected parallel to the impact surface to illuminate horizontal slices of the ejecta curtain (see Fig. 1), which are then recorded by cameras. The locations of individual particles determined are photogrammetrically, counted, and tracked in subsequent frames in a Lagrangian fashion to determine velocities. Since the particles themselves are directly measured in this analysis, the ejecta mass can be readily calculated and then combined with velocities to yield the ejecta mass distribution.

Analysis and Results:

The number of particles illuminated by the laser light sheet can be counted directly when the sheet thickness is tuned properly (as in Fig. 2). If “clumping” of illuminated particles occur (due to overlap) the total measured area of the illuminated clump is divided by the average area of individual particles (~3pix) to estimate the number. Since the size and density of the target material is known, the volume and mass in each successive time step can be calculated from this number density.

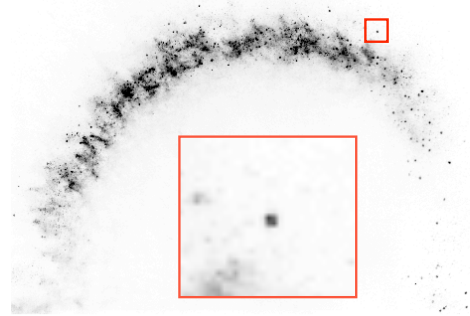


Figure 2. Example top-view image of the laser-illuminated ejecta “slice” (image is inverted for clarity). A particle is identified by the red box and zoomed in (center box).

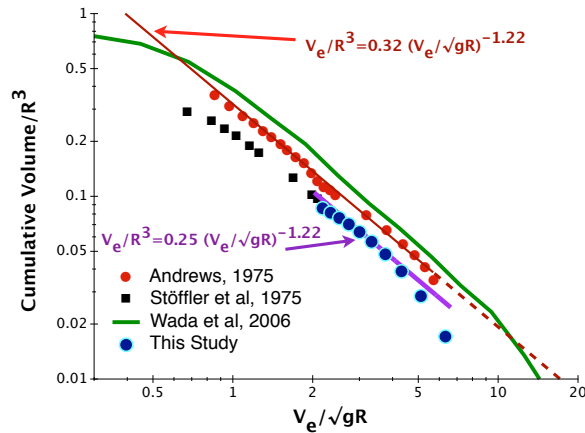


Figure 3. Cumulative non-dimensional volume of ejecta with higher velocity. Blue points correspond to calculated volume; trendline in purple. Due to the thickness of the laser sheet, low-velocity materials may be over counted. This will be optimized in future experiments. For comparison, trends from explosion data in sand (red, from [Andrews, 1975]) and data for hypervelocity impacts into sand (from [Stöffler et al, 1975]) are shown.

To compare to prior studies, we calculate the cumulative volume of ejecta with higher velocity by fitting a curve to the discrete volumes at each time step and integrating (Fig. 3). Our data closely align with the lower-speed material examined in an impact ejecta ballistic sedimentation study by Stöffler et al., 1975 but contrast slightly with the explosion data commonly used as the canonical volume line for impact studies). This study also permits the measurement of incremental (or time-resolved) ejected mass (scaled to the projectile mass) as a function of velocity and launch time (Fig. 4).

Conclusions: Initial results compare well to prior experiments and accepted scaling laws, validating the proof of concept. The technique reveals the details of early-stage excavation when ejecta is moving at hundreds of meters per second, and has wide application to the distribution of material on planetary bodies. We will apply these new data to the measured ejecta mass distributions from the Deep Impact mission and impact onto A2/Linear. Future work will extend this analysis of ejecta distributions to oblique impacts.

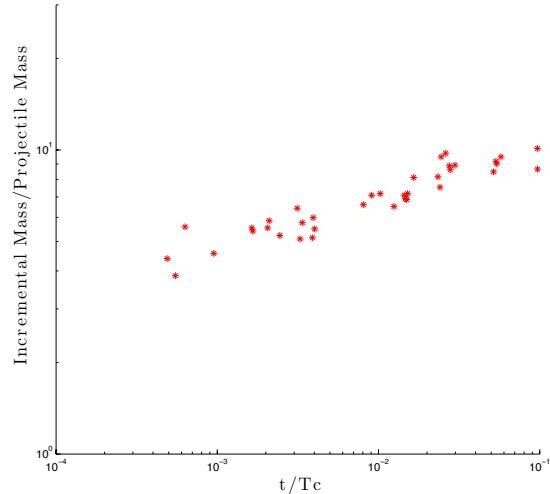


Figure 4. Incremental (time-resolved) mass ejected, scaled to projectile mass, as a function of time after impact (scaled to the T_c , the time of total crater formation).

References:

- [1] Hainaut, O.R., et al. (2012) A&A 537, A69.
- [2] Kleya, J., et al. (2013) A&A 549, A13.
- [3] Housen, K.R., et al. (1983) JGR 88, 2485–2499.
- [4] Andrews, R.J. (1974) AFRL TR 74-314.
- [5] Stöffler, D., et al. (1975) JGR 80, 4062–4077.
- [6] Oberbeck, V.R., and Morrison, R.H. (1976) LPSC Proc. Vol. 7, 2983–3005.
- [7] Schultz, P.H. (1999) LPSC Vol. 30, N. 1919.
- [8] Anderson, J.L.B., et al. (2003) JGR (Planets) 108, 5094.
- [9] Anderson, J.L.B., and Schultz, P.H. (2006) IJIE 33(1-12), 35–44.
- [10] Hermalyn, B., et al. (2012) LPSC Vol. 43, N. 2022.